Origin of induced Sn magnetic moments in thin Fe/Cr/Sn/Cr multilayers

Sanghamitra Mukhopadhyay and Duc Nguyen-Manh
Department of Materials, University of Oxford, Parks Road, Oxford OX1 3PH, United Kingdom
(Received 18 February 2002; revised manuscript received 31 May 2002; published 14 October 2002)

The origin of magnetic moment induced on one monolayer of Sn embedded within thin layers of Cr in Fe/Cr/Sn/Cr and Cr/Sn multilayers is investigated by first-principle spin-polarized electronic structure calculation. The structures consist of 1.15 nm (8 monolayers) and 1.3 nm (9 monolayers) of Fe, and 0.86 nm (6 monolayers) to 2.4 nm (17 monolayers) of Cr. The position of the Sn monolayer in Cr is either symmetric or asymmetric with respect to the Fe layers. It is found that in all these multilayers the Sn atoms get a small magnetic moment which is predominantly $5d$ in character. This is induced by the exchange interaction with the $3d$-Cr orbitals at the Cr/Sn interfaces. We find that the presence of Fe layers reduces the magnetic moment of Cr atom at the Cr/Sn interface, and therefore the induced magnetic moment on Sn atom decreased from $0.067\mu_B$/atom in Cr/Sn structure to $0.044\mu_B$/atom in Fe/Cr/Sn/Cr structure. These predictions are in strong correlation with Mössbauer observations at the ^{119}Sn site: the measured hyperfine field which in turn is affected by magnetic moment of surrounding Cr atoms, decreases from 13 T for Cr/Sn to 2 T for Fe/Cr/Sn/Cr multilayers. It is also found that the magnetic moment of a Cr atom depends strongly on its distance from the Fe layer, and therefore the induced magnetic moment of Sn is also influenced by the thickness of Cr multilayers. Our results show that the magnetic moments on Cr sites decrease smoothly away from the Fe layer and then increase abruptly at the Cr/Sn interface.

DOI: 10.1103/PhysRevB.66.144408 PACS number(s): 75.70.Cn, 71.15.Mb, 73.20.At, 71.15.Ap

I. INTRODUCTION

The magnetic properties of Fe/Cr multilayers are extremely useful technologically[1] and raise interesting fundamental questions.[2,3] Many experimental studies have been reported[4,5] on this system. However, there is no reliable method to study the magnetic moments of thin Cr layers in Fe/Cr multilayers. Results of perturbed angular correlation[6] and neutron diffraction experiments[7] are not conclusive for thin Fe/Cr multilayers.[8] Another technique, scanning electron microscopy with polarization analysis, has been used for thin Cr layers, but is unsuitable for epitaxial Fe/Cr multilayers since Fe/Cr wedges are used in this experiment.[8] Recently, epitaxial Fe/Cr/Sn/Cr multilayers were grown to investigate the magnetic moment of thin Cr layers embedded within Fe layers by introducing a monolayer (ML) of ^{119}Sn probe which could be studied by Mössbauer experiment.[9] The Fe/Cr system has been studied theoretically.[10–13] A thorough recent review by Fishman[8] may be of interest to readers. The Cr/Sn, and Fe/Cr/Sn systems, however, remain relatively unexplored. A good understanding of the novel Fe/Cr/Sn/Cr system is, therefore, required.

It was expected that the magnetic moments of Cr layers would not be affected by the presence of nonmagnetic Sn atoms in the Mössbauer experiment.[14,15] A large hyperfine field of 13 T was, however, observed at the Sn nuclear sites in Cr(0.5 nm)/Sn(1 ML) multilayers.[14,15] A strong enhancement of the hyperfine field up to 12.9 T was also observed[16] in a presurface zone of the bulk, single-crystal (110)Cr, implanted with ^{119}Sn. In both the cases the hyperfine fields were attributed to the neighboring Cr atoms, and were large compared to that of approximately 6 T for a single Sn impurity in bulk Cr.[17] In the Fe/Cr/Sn/Cr multilayers the hyperfine field decreased dramatically[9,18] to 2 T for thin (0.5 nm wide) Cr layers. It was not clear whether any magnetic moments were induced on the Sn atoms, and in turn convoluted the results for the Cr atoms. In this paper we will show that the position of the Sn atom at the substitutional site of bcc Cr(100) is also important along with the strong hybridization between Sn and Cr to explain the experimental results mentioned above.

First-principle electronic structure calculations for the Cr/Sn multilayer have been done by tight-binding linear muffin-tin orbital (TB LMTO)[19,20] and full-potential linear augmented plane-wave[21] methods. It was shown in these spin-polarized calculations that the magnetism of the Cr layers adjacent to the Sn layers was influenced by the interface states at the Sn/Cr interface. The reduction of the symmetry is also expected to alter the magnetism of the Cr layer adjacent to the Sn layer compared to that of bulk Cr. Further, the magnetic structure of the Cr/Sn layers is influenced by ferromagnetic Fe when these are embedded within Fe layers. Momida and Oguchi[21] obtained theoretically large hyperfine fields at Sn sites for Fe/Cr/Sn/Cr multilayers, which is consistent with the experimental results.[9] However, these authors reported that ''despite such a large field at the Sn nuclear site, the total spin moment of Sn is completely zero.'' In their work Momida and Oguchi[21] discussed only about $5s$-$5p$ orbitals of Sn. It is usual practice[22] to include only the $5s$-$5p$ orbitals as the basis set for Sn to explain band magnetism in ternary intermetallic systems of transition metals and Sn. In this context, it is interesting to see the effect of the $5d$ orbitals of Sn in the Fe/Cr/Sn structure where Cr/Sn forms a bcc lattice,[14] and antiferromagnetic Cr atoms which have $3d$ electrons are the nearest neighbors of Sn atoms. In this paper we show that the inclusion of the $5d$ orbitals of Sn leads to magnetic moment on the Sn atoms. The nature of variation of this magnetic moment is similar to the observed magnetic hyperfine field of Sn in Cr/Sn and Fe/Cr/Sn systems[9,14,15] which is important in the light of a recent in-

teresting observation[23] of a strong correlation (not necessarily linear) between the experimental hyperfine field and the calculated magnetic moment.

The variation of magnetic moment across the thickness of a Cr layer is a complex phenomenon, and depends on the overall width of the Cr layer,[24] proximity to other species[25] as well as the position of the Cr layer at which the moment is measured.[23] In the scope of the present work it is also important to find out how the magnetic moment of Cr is influenced by Sn in Cr/Sn and Fe/Cr/Sn/Cr multilayer structures. Two major cases arise from symmetry considerations, namely, the symmetric and the asymmetric positions of a Sn ML in the multilayers, which are studied here.

In Sec. II we discuss the computational details of the calculations. In Secs. III and IV results for the symmetric and asymmetric multilayer structures. Conclusions of our study are summarized in Sec V.

II. COMPUTATIONAL DETAILS

The electronic structure of Fe/Cr/Sn multilayers was computed using self-consistent spin-polarized supercell energy-band calculations within the local spin-density approximation to density-functional theory.[26] We used the TB-LMTO method within the atomic sphere approximation (ASA)[27] and the combined corrections were also taken into account. This technique was proved to be useful for studying the magnetic properties of multilayer systems.[20,28] The actual multilayer system was modeled by a $(m+n+l)$ supercell with m layers of Fe, n layers of Cr and $l=1$ layer of Sn along the (100) direction. The structures $Fe_9/Cr_3/Sn/Cr_3$, $Fe_9/Cr_4/Sn/Cr_4$, $Fe_9/Cr_8/Sn/Cr_8$, $Fe_9/Cr_{14}/Sn/Cr_2$, and $Fe_8/Cr_{15}/Sn/Cr_2$ were studied, where the subscripts give the number of MLs in the multilayer structure. Two typical superlattice structures are illustrated in Figs. 1(a) and 1(b). Sn was always taken as one ML. The position of the Sn layer varied for different sets of calculations. In these calculations we considered both Cr and Sn to have the bcc structure and the constructed supercell had tetragonal symmetry.

All our calculations were semirelativistic within the frozen core approximation.[29] The inflated muffin-tin spheres overlapped the structure of the supercell, and no empty spheres were required for space filling.[29] The atomic sphere overlaps were well within the permissible limit (16%) of the ASA. An overlap of 13% between the Sn and the Cr atoms was maintained in all our calculations. Thus, the overlap of the atomic spheres did not introduce any spurious variation of the magnetic moment. The supercell calculations were performed with a (8,8,2) **k** mesh. This corresponded to a total of 30 **k** points in the irreducible Brillouin zone. The Brillouin zone integration in **k** space was done by means of the improved tetrahedron method.[30] All the *s,p,d* partial waves were included in the basis of Cr, Fe, and Sn while for Sn we took the $4f$-orbital downfolded. It was observed that downfolding of $4f$ did not change the occupation and structure of the $l=3$ partial density of states (DOS), but downfolding of $5d$ had a dominant effect on the self-consistent results for the magnetic moments. Self-consistent calculations were performed within the accuracy of 1×10^{-2} mRy for the total energy and 8×10^{-5} electronic charge/(a.u.)^3 for the charge and spin densities.

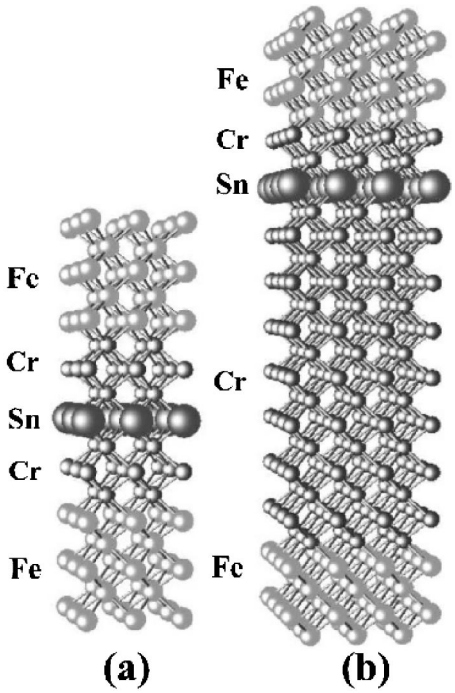

FIG. 1. (a) $Fe_9/Cr_3/Sn/Cr_3$, (b) $Fe_8/Cr_{15}/Sn/Cr_2$ multilayer structures (not to scale).

The present study was confined to thin Cr layers only, and so the spin-density wave calculations were not in the scope of the work. In order to perform the antiferromagnetic calculations we assumed that the Cr atoms of the consecutive layers had alternate spin directions, while all the Fe atoms had the same spin directions. Although at the Fe/Cr interface both ferromagnetic and antiferromagnetic coupling have been assumed as initial conditions, after the self-consistent calculations it was found that the Cr atoms were antiferromagnetically coupled with nearest-neighbor Fe atoms. Initially no exchange splitting was assumed for the Sn layer. In view of the reported dependencies of the Cr magnetic moment on the exchange correlation potential,[31–33] we assumed the Vosko-Wilk-Nusair parametrization of the Ceperly-Alder exchange correlation potential, because it produced a magnetic moment of $0.59\mu_B$/atom for bulk Cr which is close to the experimentally measured value ($0.62\mu_B$/atom) for the experimental lattice constant 2.88 Å.

Since bulk Fe and Cr are almost lattice matched, we chose the experimental value for the bulk Cr-lattice constant, 2.88 Å as the in-plane lattice constant for the case of the Fe/Cr multilayers. The out-of-plane interplanar separation for both Fe-Fe and Cr-Cr were chosen as 1.44 Å which is half the experimental bulk Cr-lattice constant. When Sn was introduced within the Cr layer, it replaced one Cr layer. In the Fe/Cr/Sn/Cr multilayer, the Cr-Sn separation was taken as 1.57 Å which is the experimentally measured distance between the Cr and Sn layers.[9] A self-consistent first-principle calculation showed that the lattice constant for bcc Sn was 3.7 Å. Thus, the interlayer separation between the Cr-Sn lay-

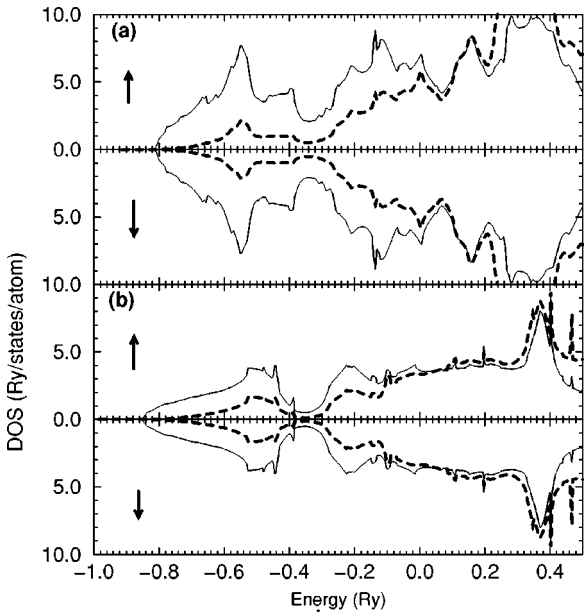

FIG. 2. DOS of (a) β Sn, and (b) bcc Sn $\uparrow$ and $\downarrow$ indicate the up and down spin, respectively. Dashed lines show $6\times$ magnified DOS of the $5d$ orbital. Energy is zero at the Fermi energy.

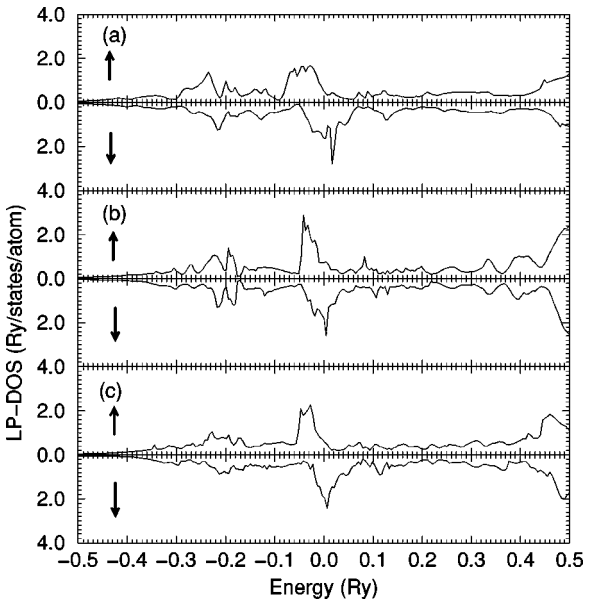

FIG. 3. LP DOS of Sn-$5d$ orbital in (a) Cr_3/Sn, (b) Cr_4/Sn, and (c) Cr_8/Sn. $\uparrow$ and $\downarrow$ indicate the up and down spin, respectively. Energy is zero at the Fermi energy.

ers was in between the Cr-Cr separation in bcc Cr and the Sn-Sn separation in bcc Sn.

III. MULTILAYERS WITH SYMMETRICALLY POSITIONED Sn LAYERS

In this section we present calculations with Sn at the mirror symmetry position in the Fe/Cr/Sn/Cr multilayer structure. In the Cr/Sn multilayer the Sn layer gets magnetic moments due to induced magnetism from interfacial Cr layers. When sandwiching Fe layers are present, we consider that these are ferromagnetically coupled across the Cr/Sn layers and modulate magnetic structure of the latter. The spin-polarized DOS along with that for the $5d$ orbital of Sn in the ground-state tetragonal, and bcc structures are shown in Figs. 2(a) and 2(b), respectively. No exchange splitting is observed in the DOS, indicating pure Sn is indeed nonmagnetic.

The spin-polarized layer projected density of states (LP DOS) for the d orbital of the Sn layer for Cr/Sn multilayers are shown in Fig. 3. Panels (a), (b), and (c) in the figure correspond to increasing thickness of the Cr layer in the sequence Cr_3, Cr_4 to Cr_8. The LP-DOS structures of Sn in multilayers differ from that of pure bulk Sn due to reduced symmetry of the interface, and bonding with interfacial Cr atoms. A clear exchange splitting for the Sn-$5d$ orbital is observed in the multilayers, which is responsible for the magnetic moment on the Sn atom. Although the splitting is relatively large, the small density of states at and below the Fermi energy leads to a small magnetic moment at a Sn site.

The magnitude of the exchange splitting depends on the number of Cr layers between the two Sn MLs in the Cr/Sn structures. The magnetic moments of Sn and the interfacial Cr layers in different structures are given in Table I along with the magnetic moment for bulk bcc Cr calculated for the same lattice constant used for Cr in the multilayer calculation. It is observed that the magnetic moments on the Sn atoms reflect the nature of magnetization of the interfacial Cr layers as assumed in the discussion of the hyperfine field on the ^{119}Sn site.[15] From the present calculations magnitude of exchange splitting is nearly the same for 3 and 8 MLs of Cr. It is coherent with experimental observations[14,15] that the hyperfine fields of Sn are nearly equal for 3 (0.5 nm), and 7 MLs (1 nm) of Cr in Cr/Sn structures. The magnetic moment on Sn atom embedding 4 MLs of Cr falls by 31% from that for 3 MLs of Cr. There is no such experiment to our knowledge for 4 MLs of Cr and the sharp reduction in the magnetic moment has not been observed so far. The two embedding Sn layers in the Cr_4/Sn structure have opposite spin polarizations (because the number of Cr layers between the Sn layers is even), which results in a reduction in the magnetic moments of both the Sn layers. If there is an odd number of intermediate Cr layers (e.g., in Cr_3/Sn), the two sandwiching Sn layers have the same spin polarization, and consequently have larger magnetic moments than in the Cr_4/Sn

TABLE I. Magnetic moment on Sn and Cr interfacing with Sn in different structures (in units of μ_B/atom).

Structures	Cr_{left}	Sn	Cr_{right}
Bulk Cr	0.59		
Cr_3/Sn	1.006	0.067	1.006
$Fe_9/Cr_3/Sn/Cr_3$	0.608	0.044	0.608
Cr_4/Sn	0.622	0.046	0.622
$Fe_9/Cr_4/Sn/Cr_4$	0.640	0.048	0.640
Cr_8/Sn	0.986	0.069	0.986
$Fe_9/Cr_8/Sn/Cr_8$	0.562	0.046	0.562
$Fe_9/Cr_{14}/Sn/Cr_2$	0.167	0.032	0.598
$Fe_8/Cr_{15}/Sn/Cr_2$	-0.143	0.016	0.582

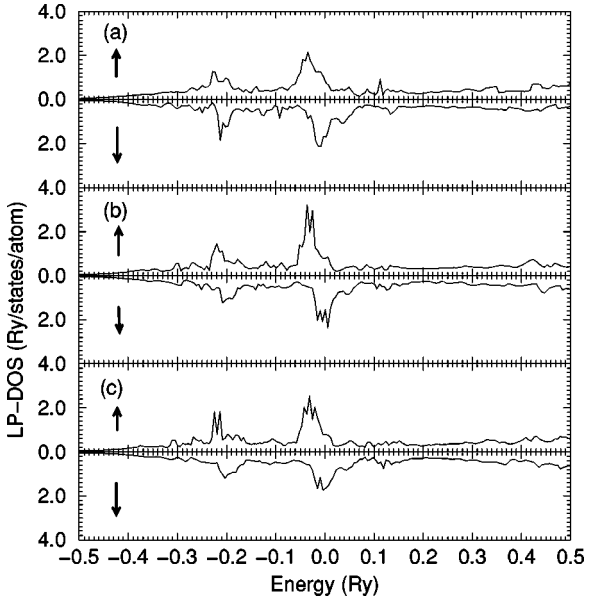

FIG. 4. LP DOS of Sn-5d orbital in (a) $Fe_9/Cr_3/Sn/Cr_3$, (b) $Fe_9/Cr_4/Sn/Cr_4$, and (c) $Fe_9/Cr_8/Sn/Cr_8$. ↑ and ↓ indicate the up and down spin, respectively. Energy is zero at the Fermi energy.

structure. The effect of this odd or even number of Cr layers in between two sandwiching Sn layers becomes important when the number of Cr layers are small and the two embedding Sn atoms share the same Cr atoms as their second-or third-nearest neighbors.

LP DOS for Sn layer for Fe/Cr/Sn/Cr multilayers are shown in Figs. 4. Panels (a), (b), and (c) in the figures correspond to increasing thickness of the Cr layer in the sequence Cr_3, Cr_4 to Cr_8. Comparing Figs. 3 and 4 for the same thicknesses of Cr, it is seen that the spin-polarized LP DOS of Sn is influenced by Fe. From Table I it is found that the magnetic moments of the Sn atoms are 34% smaller in the Fe/Cr/Sn structures than in the Cr/Sn layers when the Cr layer is 3 and 8 MLs thick. The reduction of hyperfine field from 13 T (for Cr/Sn structure) to 2 T (for Fe/Cr/Sn structure) was reported in those structures by experimental observations.[9] Therefore, there is a correlation between the calculated magnetic moment and experimental hyperfine field. However, in the light of a recent calculation[33] the amount of reduction of the magnetic moment may be dependent on the choice of exchange correlation potential. The spin polarization of the Sn atom, when it is symmetrical with the positions of the Fe layers, has the same direction as the spin polarization of the Cr atoms that are sandwiching the Sn layer, which is consistent with the observation of Mibu *et al.*[9]

TABLE II. The Contribution of different Orbitals on Magnetic Moment on Sn in different structures (in units of μ_B/atom).

Structures	5s	5p	5d	4f	Total
Cr_3/Sn	−0.009	−0.006	0.052	0.030	0.067
$Fe_9/Cr_3/Sn/Cr_3$	−0.005	−0.001	0.030	0.020	0.044
Cr_4/Sn	−0.006	−0.004	0.038	0.016	0.046
$Fe_9/Cr_4/Sn/Cr_4$	−0.007	−0.002	0.035	0.021	0.048
Cr_8/Sn	−0.010	−0.006	0.057	0.028	0.069
$Fe_9/Cr_8/Sn/Cr_8$	−0.005	−0.000	0.032	0.019	0.046
$Fe_9/Cr_{14}/Sn/Cr_2$	−0.004	−0.000	0.024	0.013	0.032
$Fe_8/Cr_{15}/Sn/Cr_2$	−0.003	−0.002	0.014	0.005	0.016

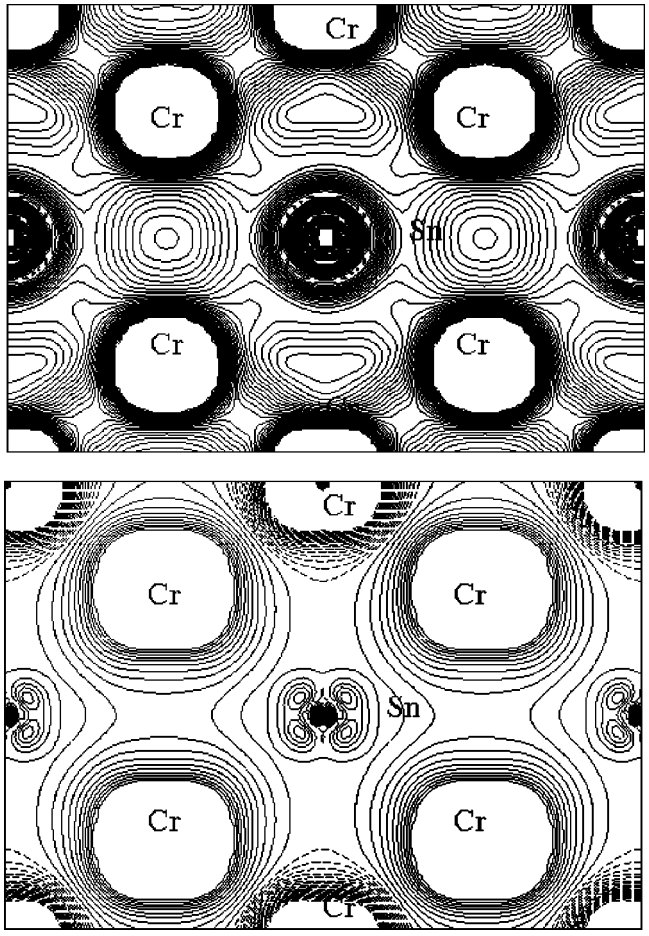

FIG. 5. (a) Charge densities (upper panel), and (b) spin densities (lower panel) in Cr_8/Sn multilayers on (110) plane, plotted in the unit of 10^{-3}electrons/(a.u.)^3. The maximum charge density of 100 occurs at the Cr sites (innermost contours). The minimum charge density of 25 occurs in between the Sn sites (innermost contours), and increases to the maximum in a step of 2. The positive and negative spin densities are shown by solid and dashed lines, respectively. The solid contour at the boundary of the positive and negative values is the zero line. Each of the positive and the negative maxima of spin density occurs at the Cr sites (innermost contours) and is +10, and −10, respectively. The steps in the plot are 1.

Contributions of various orbitals to the magnetic moment of Sn are shown in Table II. It is observed that the magnetic moment on Sn is dominated by contributions from its 5d band. Contributions from the s and p bands are one order of magnitude smaller, and are opposite in direction compared to that from the d band. These aspects are explained below in terms of charge-density distributions in the structures.

The self-consistent valence charge and spin densities for Cr_8/Sn in the (110) plane are plotted near the Cr/Sn interface in Figs. 5(a), and 5(b), respectively while those for $Fe_9/Cr_8/Sn/Cr_8$ structures are shown in Fig. 6(a), and 6(b),

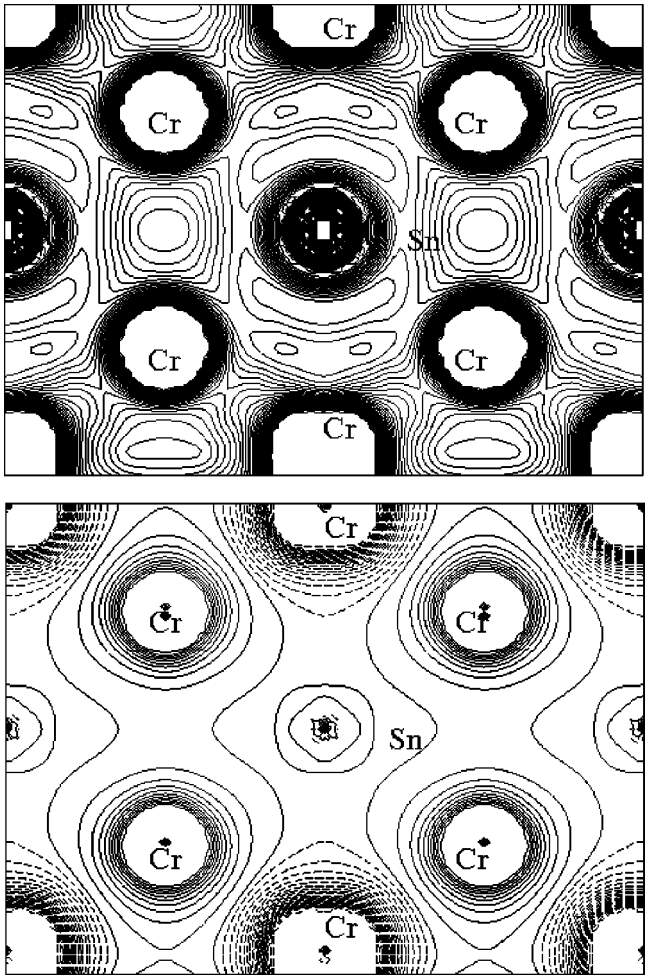

FIG. 6. (a) Charge (upper panel) and (b) spin (lower panel) densities in $Fe_9/Cr_8/Sn/Cr_8$ multilayers on (110) plane, plotted in 10^{-3} electrons/$(\text{a.u.})^{-3}$. All other attributes are the same as those of Fig. 5.

respectively. From these plots it is found that the charge is localized at the interface (I) layer between Cr and Sn, and at the next-to-the-interface (NI) layer in Cr. Although strong metallic bonds exist between Sn and its first-nearest-neighbor (1NN) Cr atoms, Sn atoms share some charge with the Cr atoms present as next-nearest neighbors to the interface. However, there is a weak directional bonding between two Sn atoms in the same layer. Charge density is smeared out from Cr atoms at the interface when the Cr/Sn structure is embedded within Fe layers. Comparing the spin densities of the two structures it is found that up-spin electrons move away from the Sn atoms towards interfacial Cr atoms in Fe/Cr/Sn/Cr, thereby reducing the magnetic moment on the Sn layer. Two opposite kinds of spin density coexist in the Sn layer. One arises due to $5d$-$3d$ hybridization between the Sn and the I Cr layers. The origin of the other is $5s,p$-$3d$ hybridization between the Sn and the NI layers.

The participation of the $5d$ orbitals of Sn occurs mainly due to the bcc structure of Cr (having electrons in its $3d$ orbitals) and Sn in these multilayers. This may be understood clearly when we compare the cases of a single substitutional Sn impurity in bulk Cr, and the Cr/Sn multilayer. In the

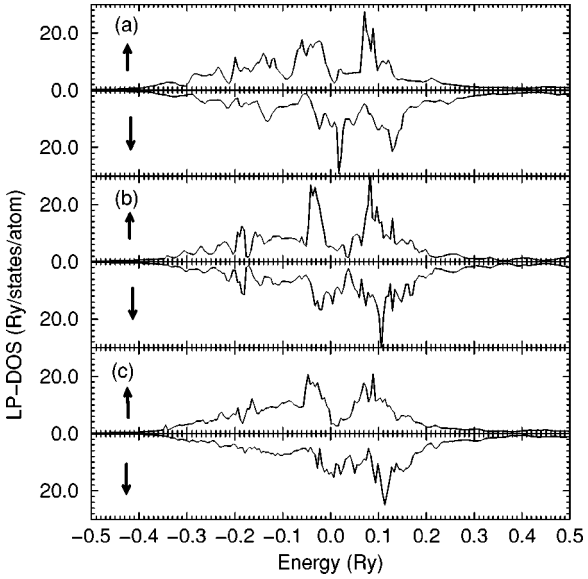

FIG. 7. LP-DOS of interfacial Cr-$3d$ orbital in (a) Cr_3/Sn, (b) Cr_4/Sn, and (c) Cr_8/Sn. The ↑ and ↓ are for the up and down spin, respectively. Energy is zero at the Fermi energy.

former, the Sn atom has eight nearest-neighbor (1NN) up-spin-polarized Cr atoms and six second-nearest-neighbor (2NN) down-spin-polarized Cr atoms. However, since the 2NN atoms are only 14% farther than the 1NN atoms in a bcc lattice, the influence of the 2NN atoms are only slightly lesser than that of the 1NN atoms. Thus, the Sn atoms in bulk Cr is effectively induced by only about two up-spin polarized Cr atoms. On the other hand in the Cr/Sn multilayer a Sn atom has eight up-spin-polarized 1NN Cr atoms, two down-spin-polarized Cr atoms, which are 17% farther from its 1NN Cr atoms, and four Sn atoms (which replace four down-

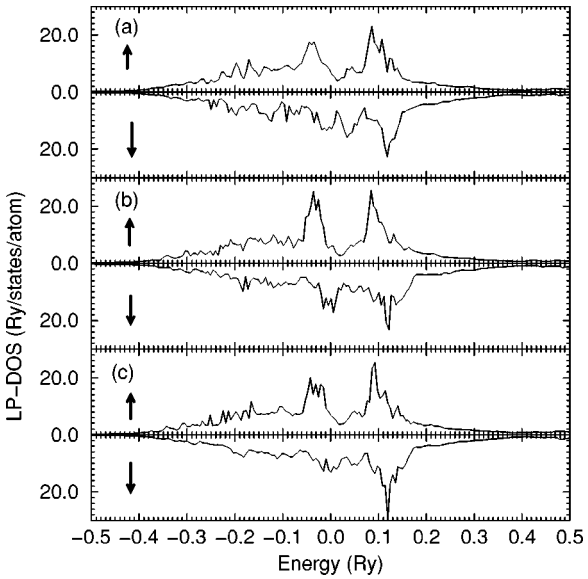

FIG. 8. LP DOS of interfacial Cr-$3d$ orbital in (a) $Fe_9/Cr_3/Sn/Cr_3$, (b) $Fe_9/Cr_4/Sn/Cr_4$, and (c) $Fe_9/Cr_8/Sn/Cr_8$. The ↑ and ↓ are for the up and down spin, respectively. Energy is zero at the Fermi energy.

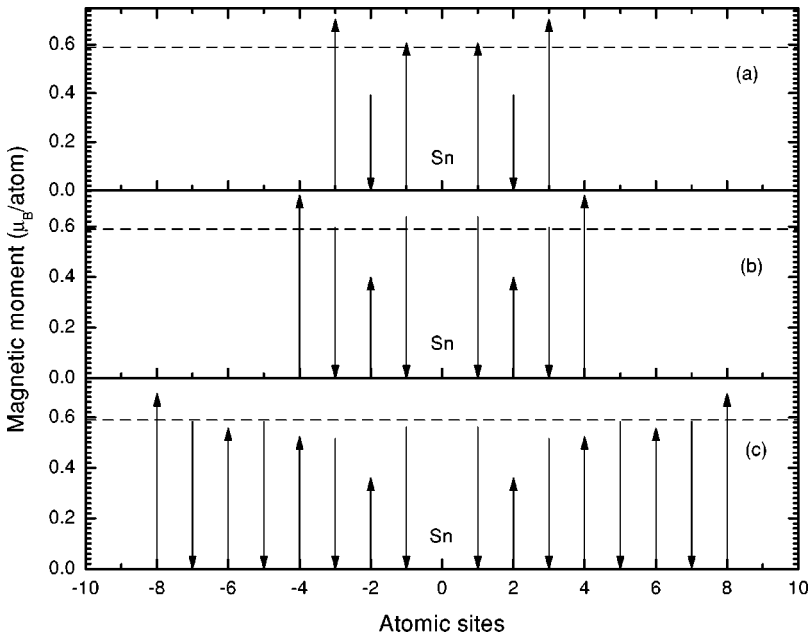

FIG. 9. Magnetic moments on Cr layers in (a) $Fe_9/Cr_3/Sn/Cr_3$, (b) $Fe_9/Cr_4/Sn/Cr_4$, and (c) $Fe_9/Cr_8/Sn/Cr_8$ structures. Sn is positioned at the origin. The up and down arrows represent up and down spins, respectively. The lengths of the arrows represent magnitudes of the magnetic moments. The dashed line shows the calculated magnetic moment of bulk Cr.

spin-polarized 2NN Cr atoms). Hence, a Sn atom in a Cr/Sn multilayer is effectively influenced by about six up-spin-polarized Cr atoms. So even by a very rough estimate, the magnetic moment induced on a Sn atom in a Cr/Sn multilayer is about three times higher than its value in bulk Cr. This is in excellent correlation with the experimentally observed values of hyperfine field: 6 T for Sn in bulk Cr,[16] and 13 T for Sn in Cr/Sn multilayers.[14,15]

From Fig. 5 it is found that an intrusion of positive spin density into the Sn layer occurs in Cr/Sn multilayer system, which indicates an increase in the magnetic moment of the *I* Cr layers. This effect enhances also the induced magnetic moment on Sn layer. From Fig. 6 it is found that the presence of Fe reduces the intrusion of positive spin density of *I* Cr layer into the Sn layer. So in case of Fe/Cr/Sn/Cr multilayers the induced magnetic moment on Sn is 34% less than that in the Cr/Sn structure. The quenching of the negative spin density occurs also in the NI Cr layers in Fe/Cr/Sn/Cr structures, but since there are only 2NI Cr atoms to influence the induced magnetic moment of Sn, the overall induced magnetic moment on Sn decreases in this structure. The electronic origin of this kind of spin density will be understood from a discussion of the LP DOS of the Cr layers.

The LP DOS for $3d$ band of the Cr layers in Cr/Sn and Fe/Cr/Sn/Cr multilayers are shown in Figs. 7 and 8, respectively. Panels (a), (b), and (c) in both the figures correspond to increasing thickness of the Cr layer in the sequence Cr_3, Cr_4 to Cr_8. The LP DOS of the Cr-$3d$ band at the interface is different from that of bulk Cr due to hybridization of the Cr-$3d$ band with Sn-$5spd$ bands. In all the structures, inter-

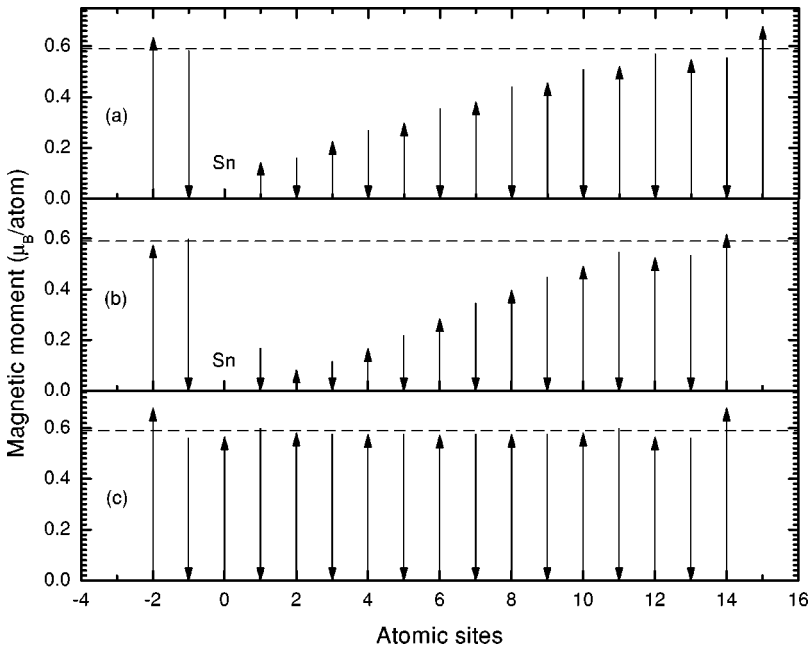

FIG. 10. Magnetic moments of Cr layers in (a) $Fe_8/Cr_{15}/Sn/Cr_2$, (b) $Fe_9/Cr_{14}/Sn/Cr_2$, and (c) Fe_9/Cr_{17}. Sn is positioned at the origin in (a) and (b). The up and down arrows represent up and down spins, respectively. The lengths of the arrows represent magnitudes of the magnetic moments. The dashed line shows the calculated magnetic moment of bulk Cr.

face states are seen within 0.1 Ry below the Fermi energy. The enhancement of the magnetic moment of the interfacial Cr is due to these interface states.[20,21] Bonding states are also prominent below 0.2 Ry of the Fermi energy, which occur due to bonding between Cr and Sn, and the peaks get smeared out in the presence of Fe.

Magnetic moment of each of the layers in the Fe/Cr/Sn/Cr structures is plotted in Fig. 9. It is seen from panels (a) and (b) that the magnetic moment of the Cr layer interfacing with Fe is $0.7\mu_B$ which is, as usual, higher[8] than that in bulk Cr ($0.59\mu_B$). Then it decreases while away from the Fe layer towards Sn layer up to NI Cr. At the interface with Sn, magnetic moment of Cr increases from that of the NI Cr layer. For $Fe_9/Cr_8/Sn/Cr_8$ structure, as seen in panel (c), the magnetic moment of Cr in the first 4 ML from the interface (including the layer interfacing with Fe) is almost constant. Then it decreases up to NI Cr and increases again at *I* Cr (with Sn) similarly as for other two structures as discussed in connection with Figs. 9(a) and 9(b). The increase in magnetic moment on the *I* Cr layer is not equivalent to that in the presence of a free surface because in such a case an increase in the magnetic moment would have occurred at the subsurface layer also. The interface states due to the difference in the atomic environment between Cr and Sn lead to the increase in the magnetic moment as calculated earlier.[20,21] The magnitude of increase in magnetic moment also depends on the number of Cr layers in between Sn and Fe.

IV. MULTILAYERS WITH ASYMMETRICALLY POSITIONED Sn LAYERS

We made self-consistent spin-polarized calculations for the Fe/Cr/Sn/Cr multilayers with the Sn layer positioned between unequally thick Cr layers, namely, for $Fe_8/Cr_{15}/Sn/Cr_2$ and $Fe_9/Cr_{14}/Sn/Cr_2$ structures. Corresponding magnetic moments are shown in Fig. 10 in panels (a) and (b), respectively. Results for the Fe_9/Cr_{17} structure are shown in panel (c) for comparison. Since the last structure can be obtained from the second one with the Sn ML replaced by a Cr ML, a comparison of magnetic moments in these two structures gives useful information about the effect of Sn in Fe/Cr multilayers. The $Fe_8/Cr_{15}/Sn/Cr_2$ structure has even number of antiferromagnetic layers in between two ferromagnetically coupled Fe layers. So this structure is energetically higher than the state where the magnetic moments of the Fe layers are antiferromagnetically coupled across the Cr/Sn structure.[10] It is found that in $Fe_9/Cr_{14}/Sn/Cr_2$ structure the magnetic moments on Cr sites decrease monotonically away from the Fe layers up to the NI Cr layer, but increases at the *I* Cr layer. The variation of the magnetic moment on the other side of the Cr/Sn interface has not been found since there are only two Cr MLs between Fe and Sn. The decrease in magnetic moment away of Cr atom from the Fe/Cr interface is also found in $Fe_8/Cr_{15}/Sn/Cr_2$ structure, but no increase at the Cr/Sn interface. No such decrease in magnetic moment is found in the Fe/Cr_{17} structure, and is consistent with reported experimental and theoretical results.[4,13] Thus the Sn ML has a significant influence on the magnetic moments of the Cr layers embedded in Fe. The decrease in magnetic moment of Cr atoms has not been seen in Cr/Sn multilayers[20] (without Fe) but an increase in magnetic moment has been found[20] at *I* Cr layer. The other embedded layers in between the Sn atoms have a constant magnetic moment. The presence of Fe in Fe/Cr/Sn/Cr multilayers modulates the magnetic moment throughout the structure. The Cr atoms at the Fe/Cr interface experience a strong exchange interaction in comparison with the Cr atoms at the Cr/Sn interfaces. This difference in the exchange interaction is responsible for the smooth decrease in magnetic moment of Cr from Fe interface to the Sn interface. We note that the calculated magnetic moment of Cr decreases at the interface of Cr/Mo in a thick multilayer.[34] A similar behavior was experimentally observed at the interface of thin (<4 nm) Cr/V samples.[35] Our self-consistent calculations for Fe/Cr/Mo/Cr multilayers with the same configuration as $Fe_9/Cr_8/Sn/Cr_8$ confirmed also the decreasing behavior of the Cr magnetic moment from the Fe interface to the Mo interface. However, the nature of such a reduction is different from that in $Fe_9/Cr_8/Sn/Cr_8$ multilayer. In the latter case, there is an abrupt increase of the magnetic moment in the Cr *I* layer. Such an increase is absent in Fe/Cr/Mo/Cr multilayer calculation. This increase is attributed to the presence of the interface states, as explained in Sec. III.

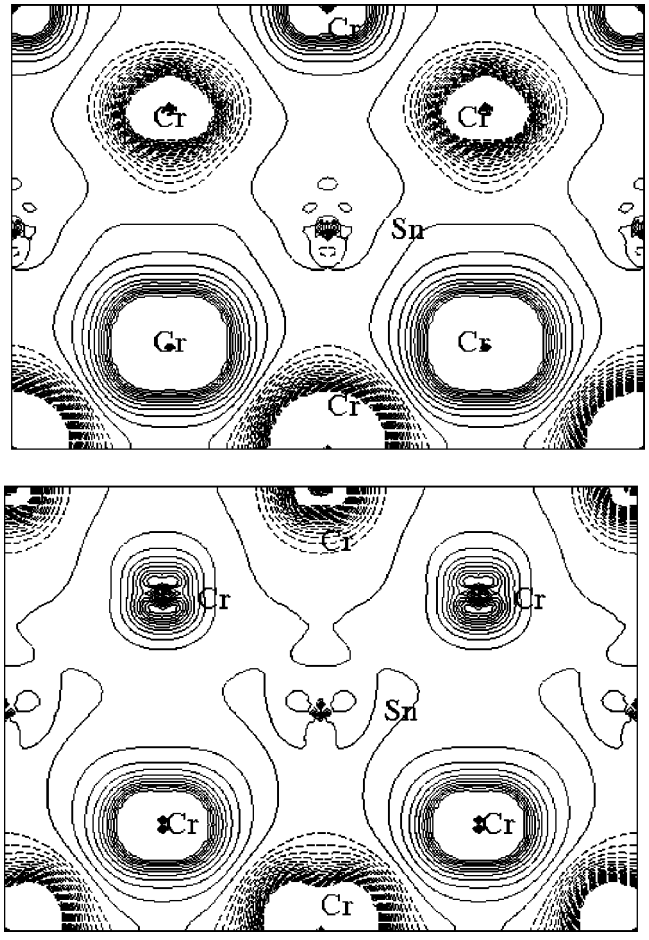

FIG. 11. Spin densities for $Fe_8/Cr_{15}/Sn/Cr_2$ (upper panel), and $Fe_9/Cr_{14}/Sn/Cr_2$ (lower panel) multilayers on (110) plane. The lower part of the figures are for the Cr layers nearer to the Fe layers. Other attributes are the same as in Fig. 6.

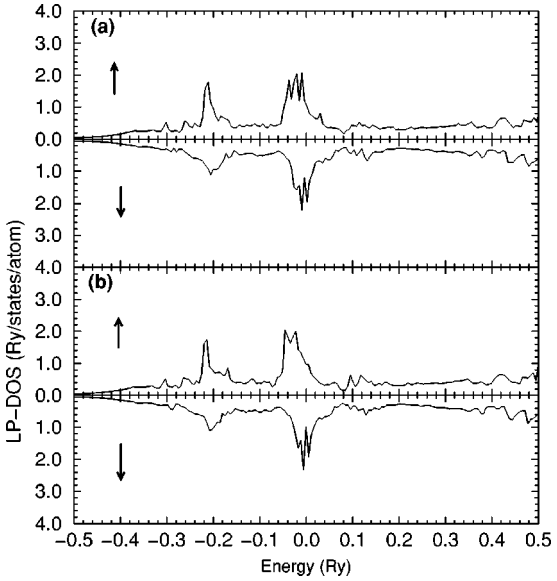

FIG. 12. LP DOS of Sn-5*d* orbital in (a) $Fe_8/Cr_{15}/Sn/Cr_2$, and (b) $Fe_9/Cr_{14}/Sn/Cr_2$. The ↑ and ↓ are for the up and down spin, respectively. Energy is zero at the Fermi energy.

There is hardly any difference in the charge distributions of the symmetric and asymmetric structures. The close proximity of the Fe layers on one side of the structures does not affect the charge distribution. Spin-density plots of these structures are shown in Fig. 11. Asymmetrical distributions of the spin density are clearly visible. It is also found that the spin density of Cr at the nearest-neighbor site of Sn depends strongly on their distance from the Fe layer. There is a ferromagnetic coupling between the Sn and the nearest-neighbor Cr layers. The antiferromagnetic coupling between the Sn and the NI Cr layer is weak, which is expected for the *d*-*d* coupling.

The electronic origin of the spin-density distributions are shown in Fig. 12 where values of LP DOS for the 5*d* band of Sn are given for the asymmetric structures. Although there is not much difference between the down-spin states of the two, dissimilarities are observed in the up-spin states indicating that the exchange splitting of Sn depends on the exchange splitting of its nearest-neighbor Cr atoms. The LP DOS for the *d*-band of both the Cr layers interfacing with Sn on the two sides are given in Fig. 13. Along with the interface states, sharp bonding and antibonding states are seen near the Fermi energy. The interfacial layers which are only 2 MLs away from the Fe layer have bonding states 0.15 Ry below the Fermi energy as seen in panels (b) and (d). The bonding states appear in the energy band 0.2–0.1 Ry below the Fermi energy both on the up-spin- and down-spin-polarized LP-DOS states and have seen also in the interface layers across the Cr/Sn interface shown in panels (a), (b), (c), and (d). The bonding states become weak on the interfacial layers which are only 2 MLs away from the Fe layer as seen in panels (b) and (d). The appearance of a sharp peak above the Fermi level of the *I* layer of Cr atoms in the $Fe_8/Cr_{15}/Sn/Cr_2$ structure as seen in Fig. 13(a) indicates antibonding with the Sn atoms. The interface states are still present in the up-spin-polarized LP DOS. The lack of bonding states in the down-spin-polarized LP DOS and the presence of occupied interface states in the up-spin-polarized LP DOS are the reasons for the occurrence of negative magnetic moment in the *I* Cr layer.

The magnetic coupling and the layer-wise variation of magnetic moments strongly depend on the quality of the interface,[4,36] and must be taken into consideration to interpret experimental observations quantitatively. Although our calculations were done assuming ideal sharp Fe/Cr interfaces which are rare in practice due to interface roughness and atomic interface intermixing between Fe and Cr, the reduction of the magnetic moment of Sn from Cr/Sn structure to Fe/Cr/Sn structures shows a strong correlation with the reduction of experimentally observed magnetic hyperfine field. This finding gives valuable insight about the role of Sn in probing magnetic moments of Cr atom in Fe/Cr multilayer systems.

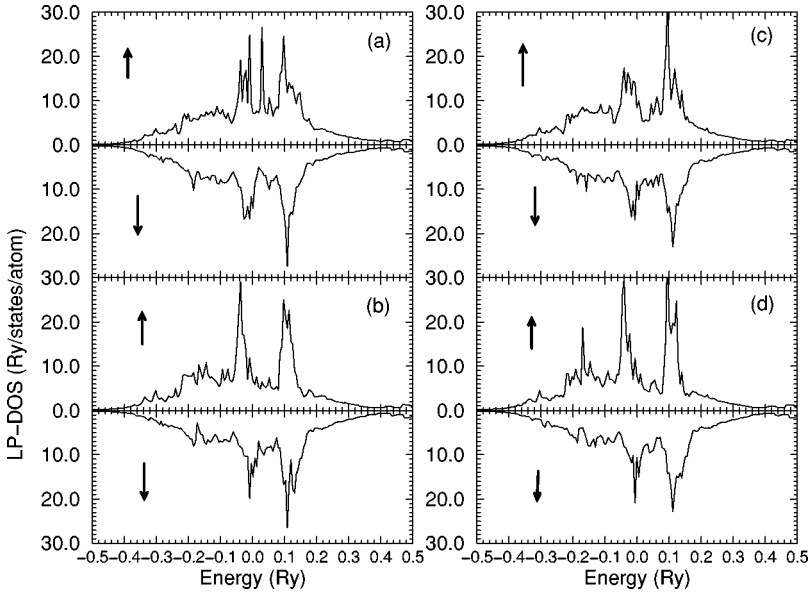

FIG. 13. LP DOS of Cr-3*d* orbital in the $Fe_8/Cr_{15}/Sn/Cr_2$ structure at the Cr/Sn interface (a) 15 ML away from Fe, and (b) 2 ML away from Fe. LP DOS of Cr-3d in the $Fe_9/Cr_{14}/Sn/Cr_2$ structure at the Cr/Sn interface (c) 14 ML away from Fe, and (d) 2 ML away from Fe. The ↑ and ↓ are for the up and down spin, respectively. Energy is zero at the Fermi energy.

V. CONCLUSIONS

In this paper we have calculated the electronic structure and magnetic properties of thin Fe/Cr/Sn/Cr multilayers using the TB-LMTO method. We draw three major conclusions from the study.

Firstly, it is shown that the magnetic properties of Sn depend on the interfacial Cr layers. A magnetic moment is induced on the Sn layer from interfacial Cr layers, which is attributed to bonding between the $5d$ orbitals of the Sn and the $3d$ orbitals of the Cr atoms. The participation of the $5d$ orbitals of Sn occurs mainly due to the bcc structure of Cr and Sn in these multilayers where a Sn atom has eight nearest-neighbor, and two second-nearest-neighbor (only 17% farther from the nearest neighbors) Cr atoms while there are only 4 second-nearest-neighbor Sn atoms. Secondly, a correlation has been found between the calculated magnetic moment on the symmetrically positioned Sn ML in Fe/Cr/Sn/Cr structure with the hyperfine field observed in the ^{119}Sn Mössbauer experiment. This implies that it is possible to use a probe Sn ML in this experiment to measure the magnetic moments in thin Cr layers. Finally, the magnetism of a Cr ML depends on its distance from the Fe layer. This produces different kinds of spin polarization on the Sn layer when its position is asymmetrical within Fe/Cr interfaces. The magnetic moment on Sn, therefore, depends on the number of Cr MLs between Fe and Sn. We find that the magnetic moment on Cr decreases away from the Fe layer, but increases abruptly at the Sn interface. The decrease is due to the differences in the exchange interactions between Fe/Cr and Sn/Cr while the increase is attributed to the presence of interface states.

We believe that the present study will be useful to gain insight into the magnetic properties of thin Fe/Cr/Sn/Cr systems where the Sn ML is used as the probe.

ACKNOWLEDGMENTS

The work presented in this paper was started when one of the authors (S.M.) was at the Inter University Consortium for DAE facilities, Indore, India. She likes to thank Professor A. Gupta, Dr. G. P. Das, and Dr. K. Mallik for useful discussions. She also thanks Professor D. G. Pettifor for reading the initial manuscript and being a kind host. Most of the calculations were done using the computer facilities of the Materials Modelling Laboratory, University of Oxford, particularly on the HP workstation which was jointly funded by the Hewlett-Packard and the HEFCE under the JERI scheme.

[1] M.N. Baibich, J.M. Broto, A. Fert, F. Nguyen, Van Dau, F. Petroff, P. Eitenne, G. Creuzet, A. Friederich, and J. Chazelas, Phys. Rev. Lett. **61**, 2472 (1988).
[2] P. Grunberg, R. Schreiber, Y. Pang, M.B. Brodsky, and H. Sowers, Phys. Rev. Lett. **57**, 2442 (1986).
[3] H. Zabel, J. Phys.: Condens. Matter **11**, 9303 (1999).
[4] P. Bodeker, A. Hucht, A. Schreyer, J. Borchers, F. Guthoff, and H. Zabel, Phys. Rev. Lett. **81**, 914 (1998).
[5] J. Meersschaut, C. L'abbe, M. Rots, and S.D. Bader, Phys. Rev. Lett. **87**, 107201 (2001).
[6] J. Meersschaut, J. Dekoster, R. Schad, P. Belien, and M. Rots, Phys. Rev. Lett. **75**, 1638 (1995).
[7] E.E. Fullerton, S.D. Bader, and J.L. Robertson, Phys. Rev. Lett. **77**, 1382 (1996).
[8] R.S. Fishman, J. Phys.: Condens. Matter **13**, R235 (2001).
[9] K. Mibu, M. Almokhtar, S. Tanaka, A. Nakanishi, T. Kobayashi, and T. Shinjo, Phys. Rev. Lett. **84**, 2243 (2000).
[10] K. Hirai, Phys. Rev. B **59**, R6612 (1999).
[11] A.M.N. Niklasson, B. Johansson, and L. Nordstrom, Phys. Rev. Lett. **82**, 4544 (1999).
[12] I. Turek, M. Freyss, P. Weinberger, D. Stoeffler, and H. Dreyssé, Phys. Rev. B **63**, 024413 (2000).
[13] K. Hirai, J. Phys. Soc. Jpn. **70**, 841 (2001).
[14] K. Mibu, S. Tanaka, and T. Shinjo, J. Phys. Soc. Jpn. **67**, 2633 (1998).
[15] K. Mibu, S. Tanaka, T. Kobayashi, A. Nakanishi, and T. Shinjo, J. Magn. Magn. Mater. **198-199**, 689 (1999).
[16] S.M. Dubiel, J. Cieślak, J. Zukrowski, and H. Reuther, Phys. Rev. B **63**, 060406 (2001).
[17] S.M. Dubiel and J. Cieslak, Phys. Rev. B **51**, 9341 (1995).
[18] K. Mibu, M. Almokhtar, A. Nakanishi, T. Kobayashi, and T. Shinjo, J. Magn. Magn. Mater. **226**, 1785 (2001).
[19] A. Gupta, A. Paul, S. Mukhopadhyay, and K. Mibu, J. Appl. Phys. **90**, 1237 (2001).
[20] S. Mukhopadhyay, G.P. Das, S.K. Ghosh, A. Paul, and A. Gupta, J. Magn. Magn. Mater. **246**, 317 (2002)
[21] H. Momida and T. Oguchi, J. Magn. Magn. Mater. **234**, 126 (2001).
[22] A. Neumann, D. Nguyen-Manh, A. Kjekshus, and A.P. Sutton, Phys. Rev. B **57**, 11 149 (1998); S.F. Matar and A. Mavromaras, J. Solid State Chem. **149**, 449 (2000).
[23] V.M. Uzdin, W. Keune, H. Schror, and M. Walterfang, Phys. Rev. B **63**, 104407 (2001).
[24] H. Xi and R.M. White, Phys. Rev. B **62**, 3933 (2000).
[25] P. Bodeker, A. Schreyer, and H. Zabel, Phys. Rev. B **59**, 9408 (1999).
[26] W. Kohn and L.J. Sham, Phys. Rev. B **140**, A1133 (1965).
[27] O.K. Andersen and O. Jepsen, Phys. Rev. Lett. **53**, 2571 (1984); R. Tank, O. Jepsen, A. Burkhardt, and O. K. Andersen, The TB-LMTO Program, Stuttgart, Germany (1995).
[28] D. Nguyen-Manh, E. Yu Tsymbal, D.G. Pettifor, C. Arcangeli, R. Tank, and O.K. Andersen, in *Microscopic Simulations of Interfacial Phenomena in Solids and Liquids*, edited by S. R. Phillpot, P. D. Bristowe, D. G. Bristowe, and J. R. Smith, Mater. Res. Soc. Symp. Proc. No. 492 (Materials Research Society, Pittsburgh, 1998), p. 319.
[29] O. K. Andersen, O. Jepsen, and M. Sob, in *Electronic Band Structure and its Applications*, edited by M. Yussouff (Springer Lecture Notes in Physics, Berlin, Heidelberg, 1987).
[30] P. Blochl, O. Jepsen, and O.K. Andersen, Phys. Rev. B **49**, 16 223 (1994).
[31] O. Gunnarsen, J. Phys. F: Met. Phys. **6**, 586 (1976).

[32] H.L. Skriver, J. Phys. F: Met. Phys. **11**, 97 (1981).
[33] S. Cottenier, B. De Vries, J. Meersschaut, and M. Rots, J. Phys.: Condens. Matter **14**, 3275 (2002).
[34] A.M.N. Niklasson, J.M. Wills, and L. Nordstrom, Phys. Rev. B **63**, 104417 (2001).
[35] M. Almokhtar, K. Mibu, A. Nakanishi, T. Kobayashi, and T. Shinjo, J. Phys.: Condens. Matter **12**, 9247 (2000).
[36] M. Kubik, T. Slezak, M. Przybylski, W. Kras, and J. Korecki, Vacuum **63**, 337 (2001).